Minireview

Structure of cation channels, revealed by single particle electron microscopy

Olga Sokolova*

Howard Hughes Medical Institute, Department of Biochemistry, Brandeis University, 415 South Street, Waltham, MA 02454-9110, USA

Received 5 December 2003; accepted 23 February 2004

First published online 15 March 2004

Edited by Fritz Winkler and Andreas Engel

Abstract A large barrier in the way to obtaining high-resolution structures of eukaryotic ion channels remains the expression and purification of sufficient amounts of channel protein to carry out crystallization trials. In the absence of crystals, the main available source of structural information has been electron microscopy (EM), which is well suited to the visualization of isolated macromolecular complexes and their conformational changes. The recently published EM structures outline native conformations of eukaryotic cation channels that until now have eluded crystallization. According to these results, homo-tetrameric K^+ channels have a distinct two-layer architecture with connectors conjoining the two layers, while the pseudo-tetrameric Ca^{2+} or Na^+ channels are more globular and have flexible surface loops, which makes the identification of subunits complicated. Subunits can be identified using atomic structure docking into the EM maps, labeling, or deletion studies.

Key words: Cation channel; Electron microscopy; Labeling

1. Introduction

Ion channels have been the focus of extensive research for more than 50 years since their role in the excitability of neuronal cells was discovered and the ionic theory of membrane excitation was established [1,2]. To date, the function of many ion channels is well understood. Moreover, recent success in obtaining atomic resolution structures of several bacterial ion channels [3–9] allows a detailed molecular characterization of ion permeation [10,11], activation [12] and gating [4,6]. An atomic structure of a more complex eukaryotic ion channel is, however, yet to be determined. High-resolution structures of mammalian ion channels are important for a deeper understanding of the various human diseases that are linked to mutations in those channels. For example, cystic fibrosis is caused by a change in the chloride permeability of cells [13], while the episodic ataxia type 1 is associated with mutations in human voltage-gated Kv1.1 channel that change its C-type inactivation [14].

A large barrier in the way to obtaining high-resolution structures of eukaryotic ion channels remains the expression and purification of sufficient amounts of active channel protein to perform crystallization. In the absence of 3D crystals, the main source of structural information has been electron microscopy (EM), which is well suited to the study of isolated macromolecular complexes and their conformational changes.

In this review I will focus on the low-resolution structures of eukaryotic cation channels derived from single particle EM studies. I aim to demonstrate that despite their resolution below 18 Å, EM structures of ion channels can reveal the location of key functional sites and provide some clues to the mechanisms of inter-subunit communications.

2. Morphology of cation channels

The first information about the overall structure of eukaryotic cation channels came from the EM images of single channels. Images of the inositol trisphosphate receptor (IP3R) [15] and *Shaker* Kv channel [16], obtained approximately a decade ago, revealed a clear four-fold symmetry of both channels. Later, the same approach was used to demonstrate that the isolated Kv channel's auxiliary β-subunit also forms a four-fold symmetric particle [17].

All K^+ channels can be recognized by certain common features: they are homo-tetramers with a monomer that consists of the ion selectivity filter, formed by a pore-lining P-loop, and two transmembrane α-helices. This minimal architecture is characteristic of the bacterial KcsA channel [3]. More complex voltage-dependent channels have extra transmembrane segments surrounding the pore (Fig. 1A). According to their specific membrane topology, K^+ channels can be separated into several groups, depending on the number of transmembrane helices [2].

The full-length sequence of Ca^{2+} and Na^+ voltage-gated channels encodes four non-identical transmembrane repeats, forming channels with a pseudo-tetrameric structure. These repeats are separated by surface loops of different length (Fig. 1B,C); some of the loops could possess glycosylation sites [18].

Cytosolic N- and C-termini participate in gating [19,20] and ligand recognition [21]; they are targets for signal transduction [22] and are thought to regulate channel activity [23]. Distal parts of N-termini of Kv channels form inactivation

*Fax: (1)-781-736 2419.
E-mail address: sokolova@brandeis.edu (O. Sokolova).

Abbreviations: EM, electron microscopy; IP3R, inositol trisphosphate receptor; RyR, ryanodine receptor; CMC, critical micelle concentration; GFP, green fluorescent protein

0014-5793/04/$30.00
doi:10.1016/S0014-5793(04)00254-6

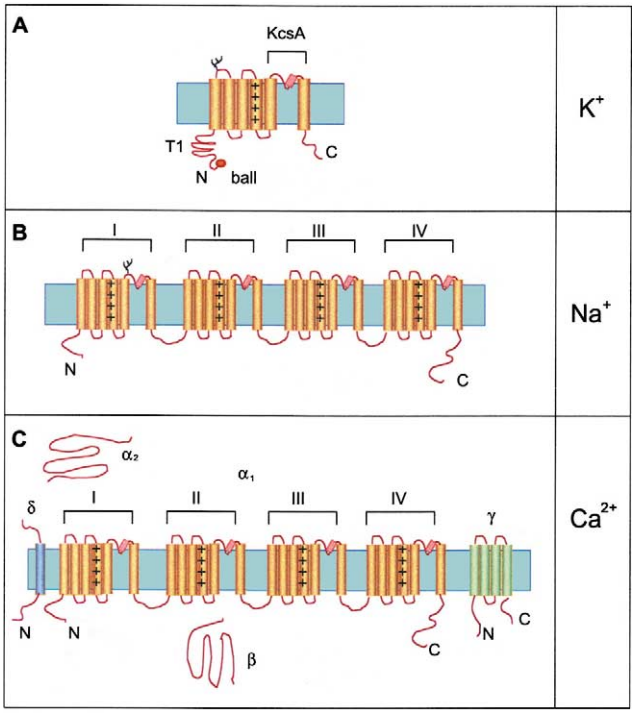

Fig. 1. Membrane topology models of cation voltage-gated channels. A: K^+ channel monomer. B: Na^+ channel. C: Ca^{2+} channel. I–IV, transmembrane helical repeats.

peptides that are necessary for the inactivation of the channel. Those flexible parts have usually been removed before crystallization in order to obtain better crystals of bacterial channel protein, thereby losing the information about their distinct conformation and location within the 3D structure of the channel. The soluble N-terminal T1 domain alone [24] and in complex with the Kvβ-subunit [25] have been crystallized in the absence of the membrane-embedded part of the channel. The interpretation of an atomic structure of the T1 domain at 1.55 Å resolution [24] suggested that the N-terminal inactivation peptide of the Kv channel is too large to proceed through the 3 Å wide opening in the center of the T1 tetramer. This observation gave rise to the hypothesis of the so-called hanging gondola [26]; its authors proposed that in order to provide access for the inactivation peptide to the pore, the T1 domain must be separated from the membrane-embedded domain similar to a hanging gondola.

3. Domain organization

Several newly published EM structures at relatively low resolution (from 35 Å to 18 Å) outline native conformations of eukaryotic cation channels. According to those studies, different cation channels could be separated into two groups, depending on their transmembrane topology.

3.1. *Channels with homo-tetrameric structure (all K^+ and some Ca^{2+} channels)*

The typical eukaryotic homo-tetrameric cation channel (Fig. 2A) has a two-layer architecture with a cytoplasmic and a membrane-embedded domain. The membrane-embedded domain accommodates the pore complex and other transmembrane segments, including the voltage sensor; in glycosylated channels it forms a square of about 10 nm wide and about 6 nm thick [21,27,28]. It is interesting to note that the membrane-embedded domains of experimentally deglycosylated channels are somewhat smaller ([29]; Sokolova, unpublished results).

The membrane-embedded domain is connected with thin linkers to the smaller cytoplasmic domain (about 6 nm wide and 4 nm thick), similar to a 'hanging gondola' [26]. The cytoplasmic domain accommodates the T1 tetramer [27] and parts of the C-termini in *Shaker* [30] or dimers of ligand binding subdomains in cGMP-gated channel [21]. The linkers are thought to be made of one or two single amino acid strands [30] and are up to 2 nm long. Ions and N-terminal inactivation peptides proceed through windows comprised by those connectors to reach the channel's pore and inactivation gate.

The two-layer architecture has also been demonstrated in other voltage-gated channels, such as Kv1.2, expressed in *Pichia pastoris* [29], mammalian Kv1.1, purified from the bovine brain [28], as well as Kv4.1, expressed in COS-1 cells [31], suggesting that this domain organization is common to most eukaryotic K^+ channels. Slim connectors are also seen in the atomic structures of the prokaryotic K^+ channels MthK [5] and KirBac 1.1 [8], confirming the universality of the two-layered K^+ channel architecture.

Similar to the K^+ channels, Ca^{2+} channels that are functional as homo-tetramers (e.g. IP3R and ryanodine receptor (RyR)) feature a two-layer architecture [32–34], and, in one case, connectors between the membrane-embedded domain and four separate cytoplasmic subdomains have been clearly seen [35]. The membrane-embedded domain of IP3R is larger than in K^+ channels – 12.6 nm wide and 7 nm thick, as determined from images of negatively stained protein [36] and a 3D reconstruction using cryo-data [33]. Each of the four cytoplasmic subdomains of IP3R is thought to contain a ligand binding site [32,35,36].

3.2. *Channels with pseudo-tetrameric structure (all voltage-gated Na^+ and Ca^{2+} channels)*

The pseudo-tetrameric cation channels are expected to contain a four-fold symmetric pore-forming domain. Indeed, the first 3D structure of a voltage-gated Na^+ channel at 19 Å resolution [37] represented a globular molecule with a square-shaped end and pseudo-tetrameric arrangement of in-

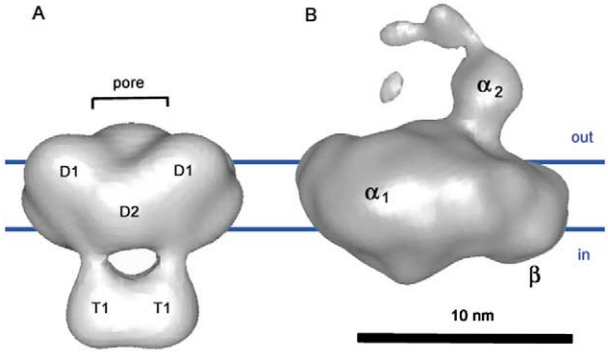

Fig. 2. 3D structures of cation channels. A: Homo-tetrameric *Shaker* K^+ channel. T1, tetramerization domain; D1, D2, subdomains that are parts of the membrane-embedded domain [29]. B: Pseudo-tetrameric L-type Ca^{2+} channel [40]. α_1, pore-forming subunit; the locations of α_2- and β-subunits have been determined using immunolabeling.

ternal cavities. Neither a two-layer architecture nor connectors were identified.

In the past 2 years, four different structures for the L-type Ca^{2+} channel have been published [38–42] (one of them is shown in Fig. 2B). The pseudo-four-fold symmetry of the pore-forming α_1-subunit was, however, not discernible in most of them. The only evidence of a possible formation of the pseudo-tetramer consisted of the four weakly separated densities in a cross-section through the putative α_1-domain of a channel dimer [42]. It is likely that the domain organization of Ca^{2+} channels is hard to determine because the additional transmembrane segments that are bound to α_1-subunit (Fig. 1C) are probably tightly packed. Also the large surface loops, connecting neighboring transmembrane repeats, and the N- and C-terminal extensions, which can occupy up to 70% of the total channel molecular mass [37], could conceal the four-fold symmetry of the pore-forming domain.

4. Domain identification within the EM structure

The identification of domains plays an important part in the interpretation of low-resolution 3D structures. Several of the most commonly used methods are discussed below.

4.1. Docking of an atomic structure

Docking of atomic structures of known parts of the channel has been used to identify the membrane-embedded and cytoplasmic domains in the 25 Å resolution 3D structure of the *Shaker* K^+ channel (Fig. 3) [27] and the 3D structures of two Kvα–β complexes at 18 Å [28] and 21 Å [29] resolution. In the last two cases, the corresponding atomic models were first band-pass filtered to a resolution comparable to that of the 3D reconstruction. This allowed a direct comparison of the atomic model to the overall EM structures. All atomic structures (KcsA – a homologue for the two pore-forming transmembrane helices [3], T1 domain [24], Kvβ-subunit [25]) were placed on the four-fold symmetry axis, taking advantage of the tetrameric structure of the ion channel. Docking also provided information about the localization of the cytosolic N- and C-termini in the *Shaker* channel [27,30], and the ligand binding sites in IP3R [32].

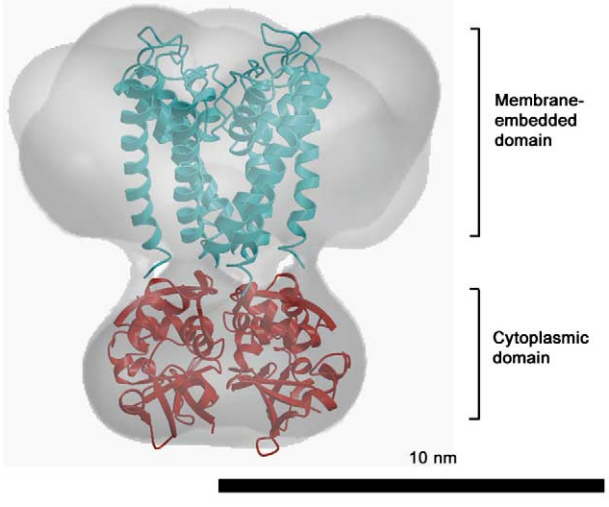

Fig. 3. Docking of atomic models of KcsA (blue) and T1 tetramer (red) into the low-resolution 3D map of *Shaker* K^+ channel.

Recently, several new atomic structures of bacterial ion channels, including the first structure of a voltage-gated channel [4,6], were published that revealed an unexpected position of some transmembrane helices (e.g. voltage sensor in [6]) within the lipid bilayer. Docking of these atomic structures into a corresponding low-resolution EM map of a full-length eukaryotic voltage-gated channel might help the interpretation of these surprising results.

4.2. Immunolabeling

Immunolabeling is a technique that is most commonly used when monoclonal antibodies against an epitope within the interpretable structure are available. A common problem in this method is the flexibility of the full-length antibody, which makes the identification of a specific binding site difficult; this problem could be overcome by using F(ab)′ fragments of the antibody. The F(ab)′ fragments are less flexible than the full-length antibody, but usually have a lower affinity. The flexibility of surface loops or cytosolic termini of the protein makes these sites undesirable for immunolabeling. Finally, unbound antibodies are usually separated from the protein–antibody complexes by gel filtration chromatography, which adds an additional step to the purification process and dilutes the protein.

Recently, antibody labeling has been performed to interpret the domain structure of the Na^+ voltage-gated channel [37]. The antibodies used in this study were directed against the C19 fragment [43] of the C-terminus of the channel. Thus, the C-terminus was shown to be a part of the larger domain that is situated in the cytoplasm adjacent to the membrane-embedded domain. In the cryo-EM study of the voltage-gated L-type Ca^{2+} channel [41], the monoclonal antibodies directed against the intracellular β-subunit and extracellular α_2-subunit were used to identify the orientation of the 3D structure within the membrane. The same antibodies directed against the β-subunit were used in another study of that channel to determine the orientation of the particles on the carbon film [38].

Monoclonal 1D4 antibodies were used to identify the location of the intracellular C-terminus of the *Shaker* K^+ channel (Sokolova, unpublished data). The apparent flexibility of the 1D4 tag, attached to the distal end of the channel's C-terminus, prevented the formation of a clear density corresponding to the bound antibody. Nevertheless, images of the channel–antibody complex localized the C-terminus near the cytoplasmic domain; that was later proved by using a deletion study [30].

4.3. Deletion or addition of protein mass

Deleting part of a protein opens up the possibility of identifying the specific location of the removed part by calculating a difference map between the full-length and truncated protein structures. This method can be used to find the location of structural elements such as cytosolic N- and C-termini. Part of the N-terminus of Kv channels forms the well-defined T1 domain, which could be crystallized in the absence of the rest of the channel [24]. Recently, some evidence that the Kv C-terminus also assumes a defined 3D structure came from physiological [23] and EM data [30]. The exact folding of the C-termini could not be established at such low resolution, but, according to both X-ray crystallography [8] and computer-generated predictions [23], the C-termini could form β-sheets.

Green fluorescent protein (GFP) is commonly used as a label to study the distribution of protein within a cell by fluorescent microscopy [44]. At the same time, GFP itself is a relatively small and compact protein of 238 amino acids, which is large enough to produce a clear density in a low-resolution EM map. Therefore, it was used as a structural marker in RyR [45–47] and Kv4.2 [31] by incorporation into the recombinant protein sequence. The advantages of GFP labeling, compared to antibody labeling, are reduced flexibility and 100% labeling of the protein.

4.4. Clusters of single molecules

To keep membrane proteins in solution, detergent must be added to form a micelle around the hydrophobic part of the molecule. Decreasing the detergent concentration in the buffer to the critical micelle concentration (CMC) forces single membrane proteins to di- or trimerize, thereby sharing a detergent micelle around their membrane-embedded domains (Fig. 4A). As a result, a cluster of several single molecules forms a 'one-dimensional' array (Fig. 4B), identifying which part of the molecule is hydrophobic and, therefore, membrane-embedded (Fig. 4C, arrows).

5. Conformational changes

All bacterial ion channels crystallized to date were in the closed state [3–7], except for MthK [5], which was crystallized

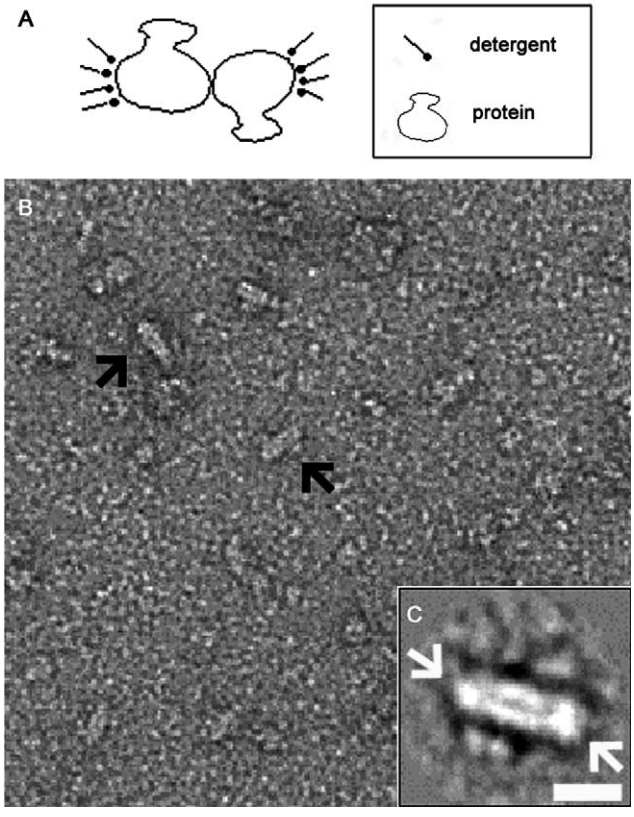

Fig. 4. Clusters of single ion channels. A: Model for cluster formation. B: Electron micrograph of *Shaker* protein in 0.5% CHAPS (the CMC of CHAPS is 6–10 mM, which is equivalent to 0.5% concentration); black arrows point to the clusters of single *Shaker* channels. C: Class average of nine selected cluster images; white arrows point to the membrane-embedded domains of two channels. Scale bar 10 nm.

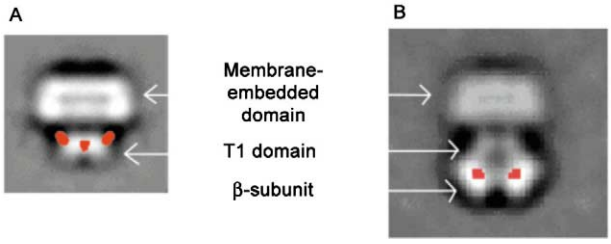

Fig. 5. Conformational changes in the C-terminus of *Shaker* upon binding of the β-subunit to the channel. A: Difference map between full-length and truncated *Shaker* (red) superimposed onto the 2D average of full-length channel. B: Difference map (red) between *Shaker* α–β complexes, containing full-length and truncated channels, superimposed onto the 2D average of full-length α–β complex. Modified from [29].

in the open state. Several hypotheses have been suggested to explain how the opening–closing and activation–inactivation of ion channels could be related to the conformational changes in different parts of the channel [4,6,8]. Single particle EM can be used to visualize larger conformational changes that may play a role in the regulation of ion channels.

The deletion study of the *Shaker* α–β complex [30] demonstrated a clear conformational change in the *Shaker* C-terminus upon binding of the β-subunit to the full-length channel (Fig. 5). The rearrangement of the C-terminus brings a large part of it from a position on the side of the T1 domain (Fig. 5A) into close contact with Kvβ (Fig. 5B). This suggested a possible mechanism for the modulation of Kv channel through the interaction of its C-termini with the β-subunit.

6. Current problems

Embedding of protein in vitreous ice preserves its structure, while the low temperature slows radiation damage that is caused by the electron beam. Unfortunately, the globular structure and relatively small size of many ion channels, the presence of detergent and, possibly, lipids, as well as the weak contrast typical for cryo-EM make it difficult to align and average images to derive a 3D structure. Negative staining produces stronger contrast but conceals the internal structure of the protein, and it may result in structural artifacts due to flattening of the protein against the carbon film and uneven staining.

The most commonly used 3D image processing methods depend on the distribution of the particle views. Random conical tilt [48] is used when particles exhibit a limited number of orientations, while angular reconstitution [49] is employed when there is a wide range of orientations. Most small ion channels, such as Kv or Na^+ channels, are often randomly oriented on the carbon film, allowing the use of angular reconstitution [21,27,32,37,41]. Larger channels, such as RyR [34], seem to prefer a small number of orientations, requiring the use of tilt experiments. Thus, the size and the shape of the molecules are determining factors for 3D image processing.

Protein purification and specimen preparation are also important for obtaining the correct 3D reconstruction of an ion channel molecule. For example, four recently published structures of the skeletal muscle L-type Ca^{2+} channel [38–42] show strikingly little agreement between them. Two structures were calculated from ice-embedded particles [39,41] and were some-

what comparable at low resolution, while the other two structures [38,40,42], derived from particles embedded in negative stain, did not show any similarity to each other or to the cryo-structures. The different purification protocols might explain such differences. Indeed, the two cryo-reconstructions were done using digitonin-solubilized protein [39,41], while the second two reconstructions used CHAPS in concentrations close to the CMC to solubilize the protein. It is known that at such concentrations CHAPS might cause aggregation of channels [41] and force the clustering of single channels in solution (Fig. 4). This aggregation may conceal the real shape of the single channel particles.

Three recent 3D structures of IP3R [32,33,35] also exhibit major discrepancies between them. The authors used two different detergents (Triton X-100 in [33,35] and CHAPS in [32]), and the purification was performed at different pH, which could result in conformational changes within the receptor [50]. Another possibility could be the weak contrast of the ice-embedded particles which can lead to erroneous alignment of the images and, consequently, unreliable 3D reconstructions.

7. Conclusions

EM and single particle analysis are versatile methods to visualize the 3D structures of macromolecular assemblies, to determine the interaction between different subunits, and to detect conformational changes. The sample preparation for EM is relatively simple, compared to X-ray crystallography or nuclear magnetic resonance. Moreover, cryo-EM opens up the possibility of studying macromolecules in a close to native state when embedded in vitreous ice. The advantage of ordered assemblies, such as 2D crystals, is that they do not need to be aligned during image processing. The first 2D crystals of a Kv ion channel in complex with a β-subunit [29] constitute a significant success on the way to determining a high-resolution EM structure of a eukaryotic ion channel. Nevertheless, the low-resolution EM studies have already provided important physiological and structural information about a wide range of cation channels.

Acknowledgements: I am thankful to Dr. N. Grigorieff for continuous attention to my work and for critical reading and comments on the manuscript and to L. Lynch for proofreading the manuscript. I also thank A. Accardi for helpful discussion and M. Wolf for the 3D map of the L-type Ca^{2+} channel.

References

[1] Hodgkin, A.L. and Huxley, A.F. (1952) J. Physiol. 117, 500–544.
[2] Hille, B. (2001) Ion Channels in Excitable Membranes, 3rd edn., Sinauer Associates, Sunderland, MA.
[3] Doyle, D.A., Morais, C.J., Pfuetzner, R.A., Kuo, A., Gulbis, J.M., Cohen, S.L., Chait, B.T. and MacKinnon, R. (1998) Science 280, 69–76.
[4] Bass, R.B., Strop, P., Barclay, M. and Rees, D.C. (2002) Science 298, 1582–1587.
[5] Jiang, Y., Lee, A., Chen, J., Cadene, M., Chait, B.T. and MacKinnon, R. (2002) Nature 417, 515–522.
[6] Jiang, Y., Lee, A., Chen, J., Ruta, V., Cadene, M., Chait, B.T. and MacKinnon, R. (2003) Nature 432, 33–41.
[7] Nishida, M. and MacKinnon, R. (2002) Cell 27, 957–965.
[8] Kuo, A., Gulbis, J.M., Antcliff, J.F., Rahman, T., Lowe, E.D., Zimmer, J., Cutherson, J., Ashcroft, F.M., Ezaki, T. and Doyle, D.A. (2003) Science 300, 1022–1926.
[9] Dutzler, R., Campbell, E.B. and MacKinnon, R. (2003) Science 300, 108–112.
[10] Morais-Cabral, J.H., Zhou, Y. and MacKinnon, R. (2001) Nature 414, 37–42.
[11] Berneche, S. and Roux, B. (2001) Nature 414, 73–77.
[12] Silvermann, W.R., Roux, B. and Papazian, D.M. (2003) Proc. Natl. Acad. Sci. USA 100, 2935–2949.
[13] Pilewski, J.M. and Frizzell, R.A. (1999) Physiol. Rev. 79, S215–S255.
[14] Lehmann-Horn, F. and Jurkat-Bott, K. (1999) Physiol. Rev. 79, 1317–1372.
[15] Chadwick, C.C., Saito, A. and Fleischer, S. (1989) Proc. Natl. Acad. Sci. USA 87, 212–2136.
[16] Li, M., Unwin, N., Stauffer, K.A., Jan, Y.-N. and Jan, L. (1994) Curr. Biol. 4, 110–115.
[17] van Huizen, R., Czajkowsky, D.M., Shi, D., Shao, Z. and Li, M. (1999) FEBS Lett. 457, 107–111.
[18] James, W.M. and Agnew, W.S. (1987) Biochem. Biophys. Res. Commun. 148, 817–826.
[19] Hoshi, T., Zagotta, W.N. and Aldrich, R.W. (1990) Science 250, 533–538.
[20] Jerng, H.H. and Covarrubias, M. (1997) Biophys. J. 72, 163–174.
[21] Higgins, M.K., Weitz, D., Warne, T., Schertler, G.F.X. and Kaupp, U.B. (2002) EMBO J. 21, 2087–2094.
[22] Kim, E. and Sheng, M. (1996) Neuropharmacology 35, 993–1000.
[23] Ju, M., Stevens, L., Leadbitter, E. and Wray, D. (2003) J. Biol. Chem. 278, 12769–12778.
[24] Kreusch, A., Pfaffinger, P.J., Stevens, C.F. and Choe, S. (1998) Nature 392, 945–948.
[25] Gulbis, J.M., Zhou, M., Mann, S. and MacKinnon, R. (2000) Science 289, 123–127.
[26] Kobertz, W.R. and Miller, C. (1999) Nat. Struct. Biol. 6, 1122–1125.
[27] Sokolova, O., Kolmakova-Partensky, L. and Grigorieff, N. (2001) Structure 9, 215–220.
[28] Orlova, E.V., Papakosta, M., Booy, F.P., van Heel, M. and Dolly, J.O. (2003) J. Mol. Biol. 326, 1005–1012.
[29] Parsej, D.N. and Eckhardt-Strelau, L. (2003) J. Mol. Biol. 333, 103–116.
[30] Sokolova, O., Accardi, A., Gutierrez, D., Lau, A., Rigney, M. and Grigorieff, N. (2003) Proc. Natl. Acad. Sci. USA 100, 12607–12612.
[31] Kim, L.A., Furst, J., Gutierrez, D., Butler, M.H., Xu, S., Goldstein, S.A. and Grigorieff, N.T. (2004) Neuron 415, 13–19.
[32] Serysheva, I.I., Bare, D.J., Ludtke, S.J., Kettlun, C.S., Chui, W. and Mignery, G.A. (2003) J. Biol. Chem. 278, 21319–21322.
[33] Jiang, Q.-X., Thrower, E.C., Chester, D.W., Ehrlich, B.E. and Sigworth, F.J. (2002) EMBO J. 21, 3575–3581.
[34] Orlova, E.V., Serysheva, I.I., van Heel, M., Hamilton, S.L. and Chiu, W. (1996) Nat. Struct. Biol. 3, 547–552.
[35] da Fontesca, P.C.A., Morris, S.A., Nerou, E.P., Taylor, C.W. and Morris, E.P. (2003) Proc. Natl. Acad. Sci. USA 100, 3936–3941.
[36] Hamada, K., Miyata, T., Mayanagi, K., Hirota, J. and Mikoshiba, K. (2002) J. Biol. Chem. 277, 21225–21228.
[37] Sato, C., Ueno, Y., Asai, K., Takahashi, K., Sato, M., Engel, A. and Fujiyoshi, Y. (2001) Nature 409, 1047–1051.
[38] Murata, K., Narumasa, O., Kuniyasu, A., Sato, Y., Nakayama, H. and Nagayama, K. (2001) Biochem. Biophys. Res. Commun. 282, 284–291.
[39] Serysheva, I.I., Ludtke, S.J., Baker, M.R., Chiu, W. and Hamilton, S.L. (2002) Proc. Natl. Acad. Sci. USA 99, 10370–10375.
[40] Wang, M.-C., Velarde, G., Ford, R.C., Berrow, N.S., Dolphin, A.C. and Kitmitto, A. (2002) J. Mol. Biol. 323, 85–98.
[41] Wolf, M., Eberhart, A., Glossmann, H., Striessnig, J. and Grigorieff, N. (2003) J. Mol. Biol. 332, 171–182.
[42] Wang, M.C., Collins, R.F., Ford, R.C., Berrow, N.S., Dolphin, A.C. and Kitmitto, A. (2004) J. Biol. Chem. 279, 7159–7168.
[43] Sato, C., Sato, M., Iwasaki, A., Doi, T. and Engel, A. (1998) J. Struct. Biol. 121, 314–325.
[44] Daly, C.J. and McGrath, J.C. (2003) Pharmacol. Ther. 100, 101–108.
[45] Liu, Z., Zhang, J., Li, F., Chen, S.R.W. and Wagenknecht, T. (2002) J. Biol. Chem. 277, 46712–46719.

[46] Zhang, J., Liu, Z., Masumiya, H., Wang, R., Jiang, D., Li, F., Wagenknecht, T. and Chen, S.R.W. (2003) J. Biol. Chem. 278, 14211–14218.
[47] Doi, N. and Yonagawa, H. (2002) Methods Mol. Biol. 183, 49–55.
[48] Radermacher, M. (1988) J. Electron Microsc. Tech. 9, 359–394.
[49] van Heel, M., Harauz, G., Orlova, E.V., Schmidt, R. and Schatz, M. (1996) J. Struct. Biol. 116, 17–24.
[50] Worley, P.F., Baraban, J.M., Supattapone, S., Wilson, V.S. and Snyder, S.H. (1987) J. Biol. Chem. 262, 12132–12136.